

Article

Molecular Dynamics Simulation of Melting of the DNA Duplex with Silver-Mediated Cytosine–Cytosine Base Pair

Elena B. Gusarova and Natalya A. Kovaleva *

N.N. Semenov Federal Research Center for Chemical Physics, Russian Academy of Sciences, 4 Kosygin Street, Moscow 119991, Russia

* Correspondence: natykov@gmail.com

Abstract: Metal-mediated base pairs in DNA double helix molecules open up broad opportunities for biosensors based on DNA clusters with silver due to their low toxicity and applicability in drug design. Despite intensive experimental and computational research, molecular mechanisms of stabilization of a double helix by silver-mediated base pairs are mainly unknown. We conducted all-atom molecular dynamics simulations of a dodecameric DNA double helix (sequence 5'-TAGGTC AATACT-3'-3' ATCCACTTATGA-5') with either cytosine–cytosine or cytosine–Ag⁺–cytosine mismatch in the center of the duplex. We extended the previously proposed set of interaction parameters for a silver ion in the silver-mediated pair in order to allow for its dissociation. With this new potential, we studied how the addition of a silver ion could stabilize a DNA double helix containing a single cytosine–cytosine mismatch. In particular, we found out that the helix with cytosine–Ag⁺–cytosine mismatch has a greater melting temperature than the helix with cytosine–cytosine one. This stabilization effect of the silver ion is in qualitative agreement with experimental data. The central region of the duplex with cytosine–Ag⁺–cytosine mismatch (unlike with cytosine–cytosine mismatch) is stable enough to prevent bubble formation at moderate temperatures during melting. The results of this simulation can be used to devise novel metal-mediated DNA structures.

Keywords: metal-base pair; silver-mediated DNA; melting temperature; molecular dynamics



Citation: Gusarova, E.B.; Kovaleva, N.A. Molecular Dynamics Simulation of Melting of the DNA Duplex with Silver-Mediated Cytosine–Cytosine Base Pair. *Computation* **2024**, *12*, 145. <https://doi.org/10.3390/computation12070145>

Academic Editor: Claudio Amovilli

Received: 2 May 2024

Revised: 4 July 2024

Accepted: 10 July 2024

Published: 12 July 2024



Copyright: © 2024 by the authors. Licensee MDPI, Basel, Switzerland. This article is an open access article distributed under the terms and conditions of the Creative Commons Attribution (CC BY) license (<https://creativecommons.org/licenses/by/4.0/>).

1. Introduction

DNA double helix is often used in nanotechnology for a wide range of applications. One promising example is the extensive search for alternatives for hydrogen bonds (H-bonds) between complementary nitrogenous bases. An attractive approach is to create a base pair with metal cations that have a high affinity for nitrogenous bases. This approach is promising for the creation of DNA-based nanomaterials with improved thermal, mechanical and chemical properties, as well as with new functionalities [1–4]. A DNA double helix in which nucleotide bases are paired by a metal ion instead of hydrogen bonds in Watson–Crick base pairs is called metalized DNA (M-DNA) [5]. Such systems are of interest due to their potential use as sensitive and specific metal sensors and biosensors [6,7]. As a rule, the inclusion of non-canonical base pairs in homochiral or heterochiral DNA leads to a decrease in the double helix stability [8]. Such decrease depends to a large extent on the specific structure of the non-canonical base pairs, their nature, and the sequence in which they are included. In 2009, Ono and Miyake [9] described two structures with metal-mediated pairs, in particular, cytosine–Ag⁺–cytosine (C:Ag:C). Their research has opened wide opportunities for DNA nanotechnology, nanoelectronics and DNA-origami due to the high specificity of silver binding [10,11]. Silver ions have attracted special attention due to their low toxicity and applicability in drug design [12,13]. As a result, numerous studies on artificial DNA containing non-canonical base pairs with silver ions were reported [14–17]. In natural DNA, silver-mediated pairing has been explored in canonical double helices with base pair mismatches [9] and in strands without canonical pairs [18–21]. High chemical

and thermal stability of the C:Ag:C base pair was demonstrated [22–26], and the role of pH in the stability of the C:Ag:C pair was studied [27]. The effect of silver on the melting temperature of DNA double helix with cytosine–cytosine (C:C) inclusions as a complementary pair has been experimentally observed [28,29]. The melting point of an oligonucleotide with C:C mismatch is increased in the presence of silver ions in solution.

To date, a number of theoretical models of base-pairing dynamics in DNA of various degrees of detailization have been developed. These models stimulate significant progress in the field of DNA melting [30,31]. The proposed models vary from the mesoscopic level (models based on the Peyrard–Bishop (PB) model [32,33]) to the coarse-grained model (CG) with several beads per nucleotide [34]. Mesoscopic models such as the PB model and its variations use a set of effective potentials to describe the main interactions in the DNA double helix, namely the hydrogen bonds and stacking interactions [35–38]. Using the mesoscopic models, the influence of single, double, and triple mismatches on duplex stability was investigated. It was found that many combinations of multiple mismatches are surprisingly stable [39]. Melting points of sequences containing metal-mediated C:C and thymine–thymine pairs were calculated [40]. The use of a CG model, where only monovalent and divalent ions are included, allows one to reproduce experimental melting temperatures for oligonucleotides [41]. In many mesoscopic and CG models, the effective non-linear potential, Lennard–Jones potential [42–44] or Morse potential [45–47] are used to mimic hydrogen bonding to describe the melting processes.

DNA melting has also been studied by means of all-atom molecular dynamics (MD) simulation [48–50]. However, the number of all-atom MD simulation studies of DNA with metal-mediated pairs is very limited. The shortest possible Ag^+ -mediated cytosine homobase duplex, a tetramer formed by Ag^+ bridges between two DNA strands, has previously been studied [16]. The Lopez-Acevedo group reported a study of Ag^+ -paired cytosine homobase DNA strands using a combination of quantum and classical MD calculations [51]. They showed that a parallel double helix has high stability, whereas an antiparallel double helix untwists and loses its helical structure. Cytosines are paired in a transoid conformation in a parallel double helix, while in an antiparallel double helix, they are in a cisoid conformation (see Figure 1a,b). The bond in the C:Ag:C pair in the cisoid conformation is weaker than in the transoid one due to an additional hydrogen bond formed between the oxygen of one cytosine and the amino group of the complementary cytosine [51–53]. The approach developed in the works of Lopez-Acevedo et al. [51] was successfully used in the MD simulation of silver-mediated base pairing in parallel-stranded DNA [29]. However, the MD simulation of the destruction of the C:Ag:C pair is challenging to date. The potentials are usually used to describe the bond of a silver ion with the nitrogen of cytosine as a covalent bond. MD's description of a covalent bond is based on a harmonic potential that does not provide a possibility for bond breaking. Therefore, a different potential has to be used to describe the destruction of the C:Ag:C pair. One possibility is to use the Morse potential, which explicitly includes the effects of bond breaking and the existence of unbound states.

In this article, we propose to use the Morse potential to describe the bond of a silver ion with cytosine by analogy with a hydrogen bond in some mesoscopic models. We simulated an antiparallel double-stranded DNA helix with C:Ag:C mismatch. We fitted parameters of the Morse potential that reproduced the process of melting a pair mediated by silver. We obtained melting curves and estimated melting temperatures. We believe that melting temperature studies of M-DNA will certainly enhance our knowledge about DNA double helix properties associated with metal-mediated base pairs.

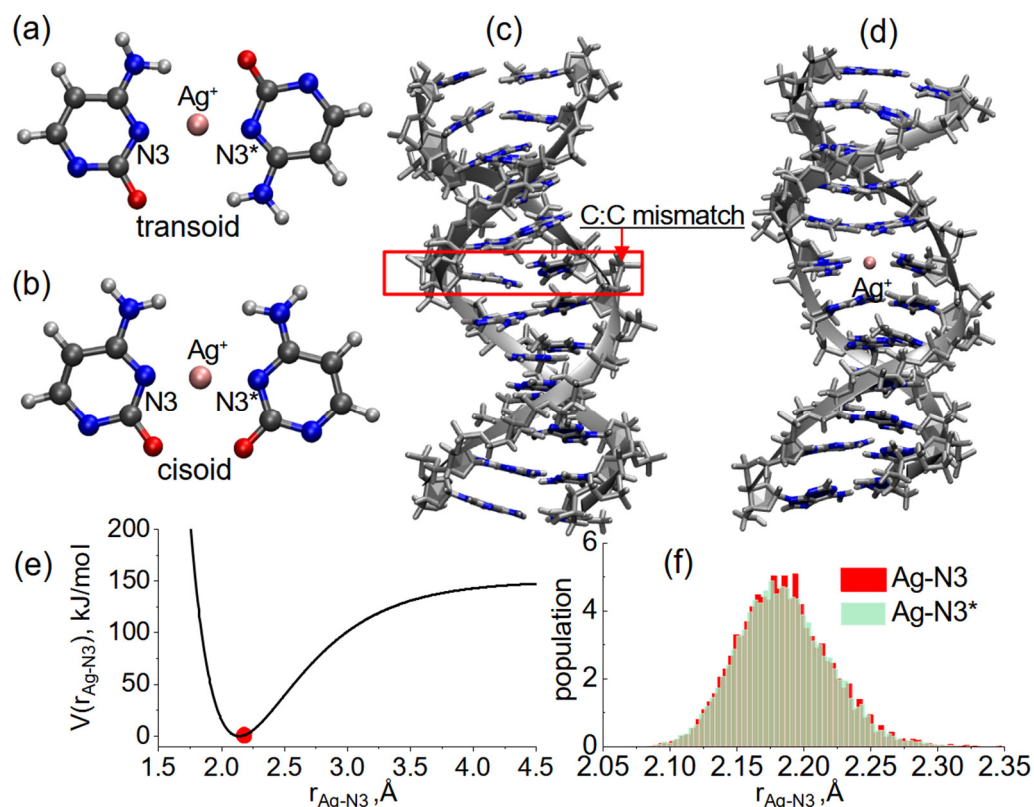


Figure 1. Structural variations for the C:Ag:C base pair: (a) transoid and (b) cisoid conformations. N3* defines the N3 atom in complementary base. DNA double helix: (c) with pure C:C mismatch and (d) with C:Ag:C formed during the classical MD. A snapshot of the double helix at $t = 100$ ns is shown. (e) The fitted Morse potential curve. The red point corresponds to the equilibrium value $r_{\text{Ag-N3}}$ in the MD simulation at a temperature of 300 K. (f) The histogram (population in percentage) of the distance between silver ion and cytosine nitrogen $r_{\text{Ag-N3}}$ at temperature 300 K. Histogram was constructed using 75 bins between 2.05 and 2.35.

2. Materials and Methods

Double-stranded DNA helix (12 base pairs) with the sequence 5'-TAGGTCAAATACT-3'-3'-ATCCACTTATGA-5' with a mismatch of complementarity in the sixth position, as C:C was considered. The initial structure was generated using the Avogadro program [54].

Initially, the DNA double helix was placed in a cubic box so that the minimum distance between the helix and the edges of the box exceeded 1 nm. Then, water molecules were added to the system. We used the TIP3P water model. To neutralize the charge of the system, 22 Na⁺ ions were added to the calculation cell. Calculations were carried out in a periodic cell using stochastic dynamics as a thermostat. Equations of motion were integrated using a leap-frog version of the Verlet algorithm. The integration step was 2 fs. Constant temperature was maintained using a stochastic thermostat, and constant pressure was maintained using a Parrinello–Rahman barostat with a time constant of 2 ps. Bonds with hydrogen atoms were constrained using the LINCS algorithm. The cutoff radii for Coulomb and van der Waals interactions were taken to be 15 Å. PME method was used to consider long-range Coulomb interactions. For MD simulation, the Gromacs 2023.1 software package [55] was used.

The parameters of potentials are a combination of the Amber99-parmbsc1 force field [56] and original parameters for Ag⁺ and cytosine interactions. Parameters of interaction between cytosine and a silver ion were taken from the literature, with some modifications as follows. Partial charges of atoms on cytosine interacting with silver ions have been corrected according to the paper [51]. The 12-6 Lennard-Jones (LJ) model was used for van der Waals interactions. The values of non-bonded interaction parameters for

the LJ potential for Ag^+ ($\sigma = 2.731 \text{ \AA}$ and $\varepsilon = 0.16316922 \text{ kJ/mol}$) and the partial charge of a silver ion ($q_{\text{Ag}^+} = 0.38272$) were taken from [57], which previously were validated for silver-mediated base pairing in double-stranded DNA in [29,51].

To simulate the bond dissociation of the silver ion from the N3 atom of cytosine, we chose the Morse potential. The Morse potential explicitly includes bond-breaking effects such as the existence of unbound states:

$$V(r) = D_e(1 - e^{-\alpha(r-r_e)})^2, \quad (1)$$

where r is the distance between N3 and Ag atoms, r_e is the equilibrium bond distance, D_e is the depth of the well, and α controls the “width” of the potential. The equilibrium bond distance $r_e = 2.14 \text{ \AA}$ is known from quantum mechanical calculations and has been successfully used in MD simulations of both transoid and cisoid pairs C:Ag:C [29,51]. The parameters of the Morse potential α and D_e were obtained as a result of an optimization procedure described below.

The optimization procedure of the Morse potential parameters consisted of two steps. At first, we determined the value of the parameter α . The idea is to keep the geometry of the C:Ag:C pair determined from quantum mechanical calculations [51], in particular, by fitting the equilibrium value of the angle N3-Ag⁺-N3* to one derived by the DFT method. To carry out this procedure, we set the parameter $D_e = 200 \text{ kJ/mol}$, which exceeds the energy of the hydrogen bond. Such a large value of D_e is required to prevent the C:Ag:C pair from spontaneous dissociation upon thermal oscillations. The initial value of parameter α was chosen so that the “width” of the Morse potential was similar to the “width” of the harmonic potential from [51].

Authors of ref. [51] introduced harmonic bonded potential as well as angular and dihedral ones in order to keep the angle N3-Ag⁺-N3* close to quantum chemical values. We used Morse potential rather than these ones and, therefore, had to optimize the “width” of the potential well.

We selected a range of values of parameter α . For each value α , we conducted an MD simulation at a temperature of 300 K with a length of 10 ns and determined the equilibrium value of the valent angle N3-Ag⁺-N3*. It turned out that $\alpha = 2.0 \text{ \AA}^{-1}$ gives the closest to quantum chemical values [51].

The next step was the parameter D_e optimization. The parameter D_e is connected with dissociation energy. We conducted a series of MD simulations heating the system as described above. We reduced the parameter D_e for each simulation. We calculated the melting curves at each value of the parameter D_e . The optimized value is $D_e = 150 \text{ kJ/mol}$. Further decrease was accompanied by the melting of the double helix with the silver ion at the same temperatures as without a silver ion. Figure 1e shows the fitted curve of the potential Morse with optimized parameters.

We conducted two types of MD simulations of a DNA double helix: equilibrium dynamics at 300 K and simulation of melting. Both simulations began with a relaxation stage followed by a production run. The relaxation stage consisted of energy minimization using the conjugate gradient method and MD simulations under conditions of constant volume (NVT ensemble) and constant pressure (NPT ensemble) at a constant pressure of 1.0 bar and temperature of 300 K for 10 ns. After relaxation, the dynamics of the system were calculated for 100 ns at a temperature of 300 K. The simulation of melting started from the configuration of the system taken from the equilibrium dynamics at 300 K. The system was heated every 20 ns with a temperature step of 10 K. MD simulations were run at temperatures ranging between 300 K and 460 K.

Based on the obtained MD trajectories, the hydrogen bonds (H-bonds) were calculated. In detecting H-bonds, the well-known geometric criterion was used: H-bond between base pairs exists if the distance between two electronegative atoms is less than 3.5 \AA and the H-bond angle is less than 30° [58].

3. Results

3.1. Dynamics and Stability of the DNA Double Helix with Either C:C or C:Ag:C Mismatch

Since we offer a new potential, we examined the stability of the dodecamer double helix in the presence of a silver ion. Therefore, after the equilibration process was completed, an MD simulation was carried out under constant temperature (300 K) and pressure (NPT) for 100 ns, of which the last 50 ns were used for analysis. The original potential was used to describe the interaction of the silver ion with cytosine atoms. These changes do not affect any other interaction parameters and should not affect the structure of the double helix outside the C:C pair mismatch. The double helix in the presence of the silver ion at 300 K was stable and had an average number of hydrogen bonds even greater than in the simulation with a C:C mismatch in the absence of a silver ion. The presence of silver ions in a system with a C:C mismatch leads to an increase in the stability of the double helix. Figure 1c,d shows typical snapshots at the end of the simulation in the absence and presence of the silver ion.

Figure 1f shows a histogram of the $r_{\text{Ag-N3}}$ distance between the silver ion and cytosine nitrogen. One can see that the MD simulation equilibrium distance $r_{\text{Ag-N3}} = 2.18 \pm 0.003 \text{ \AA}$ is scattered in close proximity around the equilibrium distance between the silver ion and cytosine nitrogen, in agreement with the literature data [51]. We also compared this equilibrium distance with the potential minimum (Figure 1e). The equilibrium value is close to the potential minimum. The displacement is due to the presence of other highly charged cytosine atoms in the immediate vicinity of the nitrogen–silver bond.

The increase in the stability of the C:C pair in the presence of the silver ion is well characterized by the $r_{\text{N3-N3}}$ distance between the N3 nitrogen atoms of cytosines in the silver-mediated pair. Figure 2a shows the $r_{\text{N3-N3}}$ distance. The average distance between N3 atoms of cytosines in the absence of silver ions at temperature 300 K the N3-N3 distance is $r_{\text{N3-N3}} = 3.97 \pm 0.27 \text{ \AA}$. In the presence of the silver ion, the N3-N3 distance is $r_{\text{N3-N3}} = 4.31 \pm 0.07 \text{ \AA}$, which is higher than in the C:C pair, but the C:Ag:C pair is more stable, as indicated by the standard deviation from the average. In this case, we observed large deformations of the C:C pair and the temporary formation of a hydrogen bond between the NH_2 group of one cytosine and the N3 atom of another cytosine. However, such a hydrogen bond turns out to be unstable.

We also calculated the local base pair parameters of the DNA double helix in the absence and presence of the silver ion. The local base pair parameters for the C:C pair are significantly different compared to adjacent pairs based on the absence of a silver ion. Local base pair parameters such as opening, shear and stretch turned out to be the most noticeable (see Figure 3a–c).

In the presence of the silver ion, the profile of shear and stretch parameters along the helix is almost flat (see Figure 3d,e). This indicates greater stability in the silver-mediated C:C pair. The non-typical value of opening is evidence of the cisoid conformation C:C pair and reflects the particular features of this non-canonical pair.

The structure of the silver-mediated pair of cytosines in the transoid and cisoid conformations can be different, as was demonstrated in [51] by the DFT method. In our case, the C:C pair is in the cisoid conformation, as in antiparallel helices. The initial cisoid conformation does not transform into a transoid one during simulation. The angles formed between the silver ion and cytosines in the coordination bond are shown in Table 1. A slight shift in the equilibrium angles is observed, indicating a displacement of the silver ion towards the cytosine oxygens.

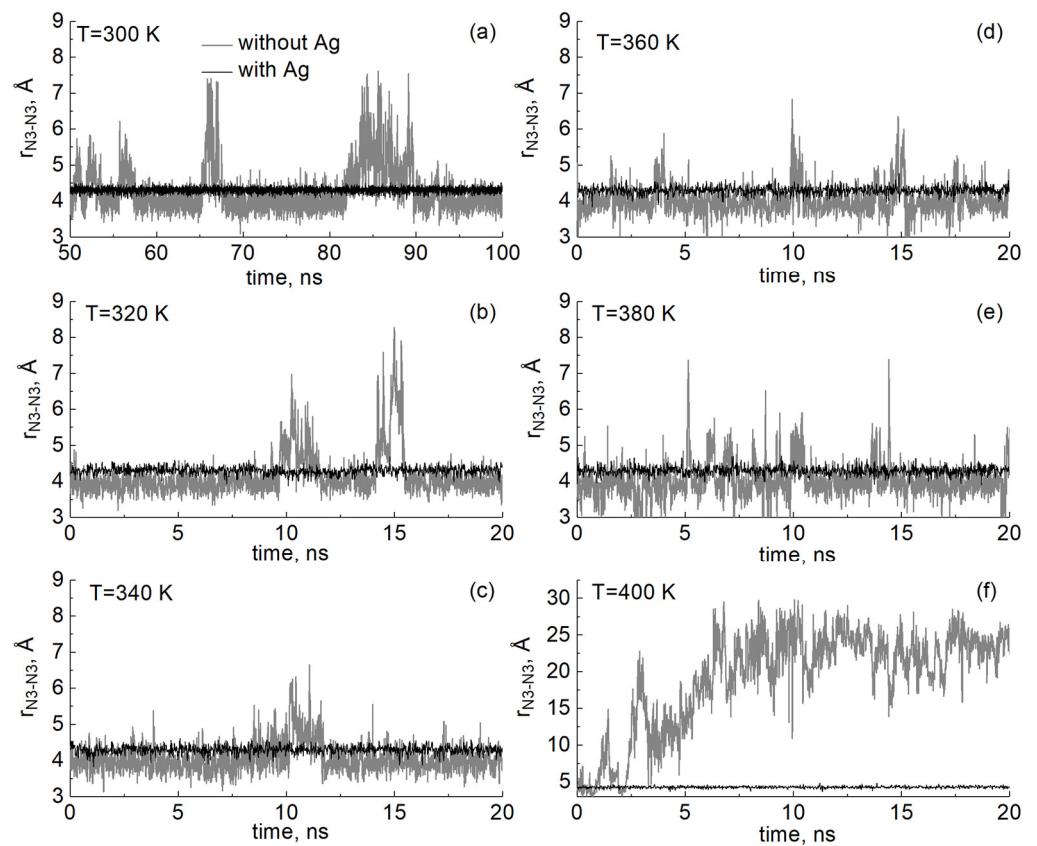


Figure 2. The distance r_{N3-N3} between nitrogen atoms N3 of cytosines in the absence of a silver ion (thick gray line) and in the presence of the silver ion (thin black line) reflects the stability of the C:C and C:Ag:C pairs: (a) A 50 ns interval at the end of the analyzed time interval for the temperature 300 K. (b–f) A 20 ns time interval for the temperatures 320 K (b), 340 K (c), 360 K (d), 380 K (e), 400 K (f).

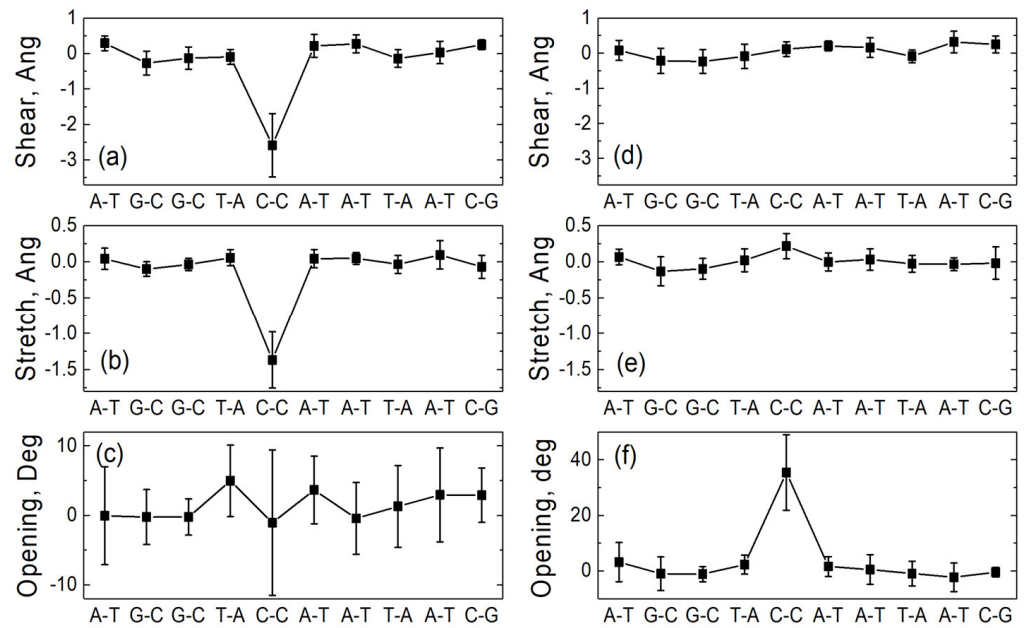


Figure 3. Local base pair parameters: shear, stretch and opening for case of absence (a–c) and presence (d–f) of the silver ion.

Table 1. Angles formed by the coordination bond between the silver ion and nitrogen N3 atom of cytosine. Standard atom notations for nucleotide bases were used.

Angle	θ , (deg)
N3-Ag ⁺ -N3*	163 ± 8
Ag ⁺ -N3-C2	103 ± 7
Ag ⁺ -N3-C4	138 ± 7

3.2. Melting of the DNA Double Helix with Either C:C or C:Ag:C Mismatch

We performed an MD simulation of DNA heating in the range from 300 to 400 K with a temperature step of 10 K. With increasing temperature, the C:C mismatch distance fluctuates strongly, which is often accompanied by the opening of a C:C pair. Figure 2 shows the r_{N3-N3} for some temperatures in the range from 300 to 400 K. At a temperature of 400 K, the C:C pair is already completely destroyed (Figure 2f). In the presence of the silver ion at a temperature of 400 K, the C:Ag:C pair is stable. The destruction of this pair coincides with the melting of the double helix at 410 K.

The maximum number of hydrogen bonds in the complementary base pairs in the sequence under consideration is 25. However, during the course of MD simulation, a smaller number of hydrogen pairs is observed as a result of base pairs fraying, a known process in MD simulations. When a DNA double helix with a C:C pair without a silver ion is heated, melting begins from the terminal base pairs of the double helix and from the C:C pair. Without a stable connection between these cytosines, the double helix forms a bubble, and three melting hot spots form in this case: two terminal pairs and the C:C mismatch. With the silver ion between two cytosines, we observe a more stable double helix, and melting occurs only from the terminal base pairs. The melting curves of the DNA double helix in the presence and absence of a silver ion are presented in Figure 4. It can be seen that in the presence of the silver ion, the melting curve is shifted towards higher temperatures, just as observed in the experiment [28].

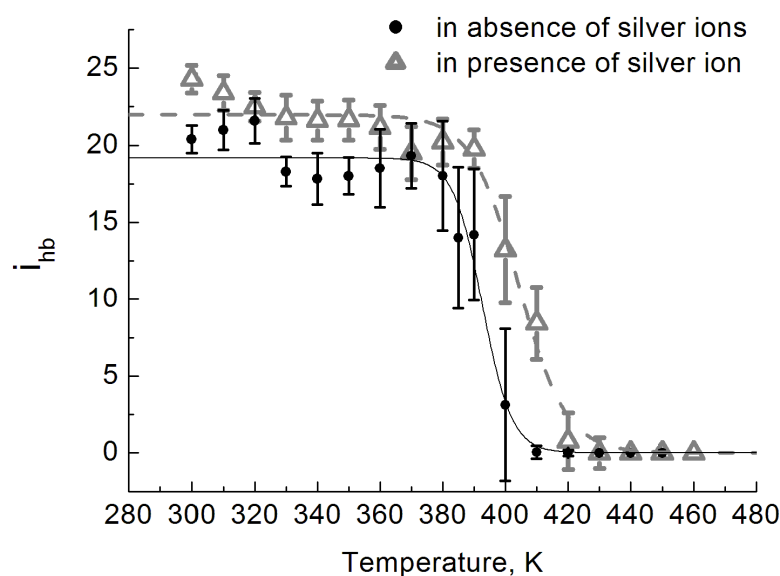
**Figure 4.** The presence of the silver ion shifts the melting curve towards higher temperatures. The temperature dependence of the number of hydrogen bonds i_{hb} without (circles) and with (triangles) silver ion is presented.

Table 2 shows the melting temperatures of the DNA double helix in the absence and presence of the silver ion. As usual for MD simulations, we obtain the higher absolute values of melting temperatures in both cases (due to the superheating, see Discussion); however, we are interested in the relative effect—the melting temperature shift due to the

silver ion presence. This shift, in our case, is 12 K, which is close to the experimental value of 7.5 K. When the DNA melts, the metal-mediated pair breaks down, and the silver ion is released into the solution. The metal-mediated pair C:Ag:C is thermally more stable than the hydrogen bonds of complementary bases, but in this case, it has one silver-mediated base pair, which is also subject to thermal destruction, as observed in the experiment [28].

Table 2. The melting temperatures for double helix in the absence and the presence of the silver ion in comparison with experimental data. The bottom row shows the shift in melting temperature due to the presence of silver ions.

Silver Ion	T_m Experiment ¹ , K	T_m MD, K
absence	299.5	392
presence	307	404
temperature shift ΔT_m	7.5	12

¹ Experimental results were taken from [28] for the same sequence as studied in this work.

4. Discussion

We took this sequence as a robust object for potential validation since its experimentally found melting point is well known in both the absence and the presence of silver ions [28]. We chose the standard antiparallel double helix since, for such objects, the MD approach is well-validated.

By introducing bond potentials to describe the coordination bond between the silver ion and cytosine, we were able to directly model the dynamics of coordinated bond breaking, which was previously impossible while treating these bonds as covalent. The main feature of our potential in comparison with early works is that the structure of the C:Ag:C pair is not fixed near the equilibrium position but can fluctuate significantly near it up to the destruction of the pair with increasing temperature. Our calculations show that the structure of the pair corresponds to the early work [51].

The discrepancies in the absolute values of melting temperatures between experiments [28] and MD simulations are common and attributed to the methodology used to simulate the nanoscale samples [59]. In MD simulations, the melting point is determined by “slow” heating; thus, the rate of temperature change compared to a real experiment is very high and can exceed the experimental value by several orders of magnitude. Since the transition does not occur instantly but requires a small (on an experimental scale) time, a shift is observed. This effect can be corrected by using Monte Carlo simulations instead of molecular dynamics, but this requires more expensive calculations. In addition, the melting temperature discrepancy is affected by the size of the simulation cell and the thermostats used. In molecular dynamics, we are dealing with a small cell, nanometers in size. In this case, the temperature change occurs instantly throughout the entire volume. In the experiment, the measured cell is macroscopic, and temperature changes inside it at the molecular level occur non-uniformly. Thus, we believe that the discrepancy between the melting temperatures in the real experiment and our results is not a disadvantage. We obtained a qualitative agreement of the melting temperature shift in the presence of a silver ion compared to the case when a silver ion is absent. In this case, we observe a satisfactory shift in the melting temperature, comparable with the experimental results.

5. Conclusions

We proposed and verified the Morse potential for the silver-mediated base pair bond that can describe the destruction of the coordination bond between cytosine and a silver ion. The verified potential parameters allowed us to reproduce the process of melting of the DNA double helix with a silver-mediated pair and the destruction of the coordination bond between the silver ion and the cytosine base with increasing temperature. The results of the simulations are in good agreement with experimental data on the melting temperature shift of the DNA double helix with a C:C mismatch in the absence and the presence of a silver ion. Since the B-form double helix is a basic building block not only in the genetic code of

living organisms but also in DNA nanotechnology, metal-mediated double helices may be used for self-assembly dynamic DNA nanomachines. Our results open new possibilities for the development of new metal-mediated 3D DNA materials with increased resistance to thermal, chemical, and possibly enzymatic degradation due to the additional stability provided by silver-mediated base pairs.

Author Contributions: Conceptualization, N.A.K.; methodology, N.A.K.; validation, E.B.G. and N.A.K.; investigation, N.A.K.; writing—original draft preparation, N.A.K.; writing—review and editing, N.A.K.; visualization, E.B.G.; supervision, N.A.K. All authors have read and agreed to the published version of the manuscript.

Funding: This research was supported by the Program of Fundamental Research of the Russian Academy of Sciences (project No. FFZE-2022-0009).

Data Availability Statement: Data are contained within the article.

Acknowledgments: The calculations were carried out in the Joint Supercomputer Center of the Russian Academy of Sciences.

Conflicts of Interest: The authors declare no conflicts of interest.

References

1. Yang, H.; Metera, K.L.; Sleiman, H.F. DNA Modified with Metal Complexes: Applications in the Construction of Higher Order metal–DNA Nanostructures. *Coord. Chem. Rev.* **2010**, *254*, 2403–2415. [[CrossRef](#)]
2. Park, K.S.; Park, H.G. Technological Applications Arising from the Interactions of DNA Bases with Metal Ions. *Curr. Opin. Biotechnol.* **2014**, *28*, 17–24. [[CrossRef](#)] [[PubMed](#)]
3. Scharf, P.; Müller, J. Nucleic Acids with Metal-Mediated Base Pairs and Their Applications. *ChemPlusChem* **2013**, *78*, 20–34. [[CrossRef](#)]
4. Swasey, S.M.; Gwinn, E.G. Silver-Mediated Base Pairings: Towards Dynamic DNA Nanostructures with Enhanced Chemical and Thermal Stability. *New J. Phys.* **2016**, *18*, 045008. [[CrossRef](#)]
5. Albarqouni, Y.; Ali, G.A.; Hairul, A.R.M.; Chong, K.F. On the Way of DNA Metallization: Principle, Methods, and Recent Applications. *Chem. Adv. Mater.* **2020**, *5*, 1–14.
6. Chatterjee, S.; Lou, X.Y.; Liang, F.; Yang, Y.W. Surface-functionalized gold and silver nanoparticles for colorimetric and fluorescent sensing of metal ions and biomolecules. *Coord. Chem. Rev.* **2022**, *459*, 214461. [[CrossRef](#)]
7. Ibrahim, N.; Jamaluddin, N.D.; Tan, L.L.; Mohd Yusof, N.Y. A review on the development of gold and silver nanoparticles-based biosensor as a detection strategy of emerging and pathogenic RNA virus. *Sensors* **2021**, *21*, 5114. [[CrossRef](#)]
8. Funai, T.; Adachi, N.; Aotani, M.; Wada, S.I.; Urata, H. Effects of metal ions on thermal stabilities of DNA duplexes containing homo- and heterochiral mismatched base pairs: Comparison of internal and terminal substitutions. *Nucleosides Nucleotides Nucleic Acids* **2020**, *39*, 310–321. [[CrossRef](#)] [[PubMed](#)]
9. Ono, A.; Cao, S.; Togashi, H.; Tashiro, M.; Fujimoto, T.; Machinami, T.; Oda, S.; Miyake, Y.; Okamoto, I.; Tanaka, Y. Specific Interactions between Silver(i) Ions and Cytosine–cytosine Pairs in DNA Duplexes. *Chem. Commun.* **2008**, *39*, 4825–4827. [[CrossRef](#)]
10. Chai, Y.; Guo, X.; Leonard, P.; Seela, F. Heterochiral DNA with Complementary Strands with α -d and β -d Configurations: Hydrogen-Bonded and Silver-Mediated Base Pairs with Impact of 7-Deazapurines Replacing Purines. *Chem. Eur. J.* **2020**, *26*, 13973–13989. [[CrossRef](#)]
11. Jash, B.; Müller, J. Metal-Mediated Base Pairs: From Characterization to Application. *Chem.–Eur. J.* **2017**, *23*, 17166–17178. [[CrossRef](#)] [[PubMed](#)]
12. Sun, Q.; Xie, X.; Song, Y.; Sun, L. A review on silver-mediated DNA base pairs: Methodology and application. *Biomater. Res.* **2022**, *26*, 9. [[CrossRef](#)] [[PubMed](#)]
13. Raju, S.K.; Karunakaran, A.; Kumar, S.; Sekar, P.; Murugesan, M.; Karthikeyan, M. Silver complexes as anticancer agents: A perspective review. *Ger. J. Pharm. Biomater.* **2022**, *1*, 6–28. [[CrossRef](#)]
14. Sinha, I.; Fonseca Guerra, C.; Müller, J. A Highly Stabilizing Silver(I)-Mediated Base Pair in Parallel-Stranded DNA. *Angew. Chem. Int. Ed.* **2015**, *54*, 3603–3606. [[CrossRef](#)] [[PubMed](#)]
15. Johannsen, S.; Megger, N.; Böhme, D.; Sigel, R.K.O.; Müller, J. Solution Structure of a DNA Double Helix with Consecutive Metal-Mediated Base Pairs. *Nat. Chem.* **2010**, *2*, 229–234. [[CrossRef](#)]
16. Mandal, S.; Hepp, A.; Müller, J. Unprecedented Dinuclear Silver(i)-Mediated Base Pair Involving the DNA Lesion 1,N6-Ethenoadenine. *Dalton Trans.* **2015**, *44*, 3540–3543. [[CrossRef](#)] [[PubMed](#)]
17. Polonius, F.-A.; Müller, J. An Artificial Base Pair, Mediated by Hydrogen Bonding and Metal-Ion Binding. *Angew. Chem. Int. Ed.* **2007**, *46*, 5602–5604. [[CrossRef](#)]

18. Swasey, S.M.; Leal, L.E.; Lopez-Acevedo, O.; Pavlovich, J.; Gwinn, E.G. Silver(I) as DNA Glue: Ag⁺-Mediated Guanine Pairing Revealed by Removing Watson-Crick Constraints. *Sci. Rep.* **2015**, *5*, 10163. [[CrossRef](#)] [[PubMed](#)]
19. Berdakin, M.; Taccone, M.I.; Pino, G.A.; Sánchez, C.G. DNA-Protected Silver Emitters: Charge Dependent Switching of Fluorescence. *Phys. Chem. Chem. Phys.* **2017**, *19*, 5721–5726. [[CrossRef](#)]
20. Megger, D.A.; Müller, J. Silver(I)-Mediated Cytosine Self-Pairing Is Preferred over Hoogsteen-Type Base Pairs with the Artificial Nucleobase 1,3-Dideaza-6-Nitropurine. *Nucleosides Nucleotides Nucleic Acids* **2010**, *29*, 27–38. [[CrossRef](#)]
21. Ramazanov, R.R.; Sych, T.S.; Reveguk, Z.V.; Maksimov, D.A.; Vdovichev, A.A.; Kononov, A.I. Ag–DNA Emitter: Metal Nanorod or Supramolecular Complex? *J. Phys. Chem. Lett.* **2016**, *7*, 3560–3566. [[CrossRef](#)] [[PubMed](#)]
22. Tanaka, Y.; Kondo, J.; Sychrovský, V.; Šebera, J.; Dairaku, T.; Saneyoshi, H.; Urata, H.; Torigoe, H.; Ono, A. Structures, physicochemical properties, and applications of T–Hg II–T, C–Ag I–C, and other metallo-base-pairs. *Chem. Commun.* **2015**, *51*, 17343–17360. [[CrossRef](#)] [[PubMed](#)]
23. Mistry, L.; El-Zubir, O.; Dura, G.; Clegg, W.; Waddell, P.G.; Pope, T.; Hofer, W.A.; Wright, N.G.; Horrocks, B.R.; Houlton, A. Addressing the properties of “Metallo-DNA” with a Ag (i)-mediated supramolecular duplex. *Chem. Sci.* **2019**, *10*, 3186–3195. [[CrossRef](#)] [[PubMed](#)]
24. Marzilli, L.G.; Kistenmacher, T.J.; Rossi, M. An extension of the role of O (2) of cytosine residues in the binding of metal ions. Synthesis and structure of an unusual polymeric silver (I) complex of 1-methylcytosine. *J. Am. Chem. Soc.* **1977**, *99*, 2797–2798. [[CrossRef](#)] [[PubMed](#)]
25. Nakagawa, O.; Aoyama, H.; Fujii, A.; Kishimoto, Y.; Obika, S. Crystallographic Structure of Novel Types of AgI-Mediated Base Pairs in Non-canonical DNA Duplex Containing 2′-O, 4′-C-Methylene Bridged. *Nucleic Acids. Chem. Eur. J.* **2021**, *27*, 3842–3848. [[CrossRef](#)] [[PubMed](#)]
26. Hossain, M.N.; Ahmad, S.; Kraatz, H.-B. Consecutive Silver (I) Ion Incorporation into Oligonucleotides containing Cytosine-Cytosine Mispairs. *ChemPlusChem* **2021**, *86*, 224–231. [[CrossRef](#)]
27. Bhai, S.; Ganguly, B. Role of pH in the stability of cytosine-cytosine mismatch and canonical AT and GC base pairs mediated with silver ion: A DFT study. *Struct. Chem.* **2022**, *33*, 35–47. [[CrossRef](#)]
28. Zhang, A.; Budow-Busse, S.; Leonard, P.; Seela, F. Anomeric and Enantiomeric 2′-Deoxycytidines: Base Pair Stability in the Absence and Presence of Silver Ions. *Chem.–Eur. J.* **2021**, *27*, 10574–10577. [[CrossRef](#)] [[PubMed](#)]
29. Schönraht, I.; Tsvetkov, V.B.; Zatsepin, T.S.; Aralov, A.V.; Müller, J. Silver (I)-mediated base pairing in parallel-stranded DNA involving the luminescent cytosine analog 1, 3-diaza-2-oxophenoxazine. *J. Biol. Inorg. Chem.* **2019**, *24*, 693–702. [[CrossRef](#)]
30. Manghi, M.; Destainville, N. Physics of base-pairing dynamics in DNA. *Phys. Rep.* **2016**, *631*, 1–41. [[CrossRef](#)]
31. Singh, A.; Maity, A.; Singh, N. Structure and Dynamics of dsDNA in Cell-like Environments. *Entropy* **2022**, *24*, 1587. [[CrossRef](#)] [[PubMed](#)]
32. Peyrard, M.; Bishop, A.R. Statistical mechanics of a nonlinear model for DNA denaturation. *Phys. Rev. Lett.* **1989**, *62*, 2755–2758. [[CrossRef](#)] [[PubMed](#)]
33. Singh, A.; Singh, N. Effect of salt concentration on the stability of heterogeneous DNA. *Phys. A* **2015**, *419*, 328–334. [[CrossRef](#)]
34. Knotts, T.A.; Rathore, N.; Schwartz, D.C.; De Pablo, J.J. A coarse grain model for DNA. *J. Chem. Phys.* **2007**, *126*, 084901. [[CrossRef](#)] [[PubMed](#)]
35. Rodrigues Leal, M.; Weber, G. Sharp DNA denaturation in a helicoidal mesoscopic model. *Chem. Phys. Lett.* **2020**, *755*, 137781. [[CrossRef](#)]
36. Zoli, M. Base pair fluctuations in helical models for nucleic acids. *J. Chem. Phys.* **2021**, *154*, 194102. [[CrossRef](#)] [[PubMed](#)]
37. Valle-Orero, J.; Wildes, A.R.; Theodorakopoulos, N.; Cuesta-López, S.; Garden, J.L.; Danilkin, S.; Peyrard, M. Thermal denaturation of A-DNA. *New J. Phys.* **2014**, *16*, 113017. [[CrossRef](#)]
38. Singh, A.; Singh, N. Pulling short DNA molecules having defects on different locations. *Phys. Rev. E* **2015**, *92*, 032703. [[CrossRef](#)] [[PubMed](#)]
39. Oliveira, L.M.; Long, A.S.; Brown, T.; Fox, K.R.; Weber, G. Melting temperature measurement and mesoscopic evaluation of single, double and triple DNA mismatches. *Chem. Sci.* **2020**, *11*, 8273–8287. [[CrossRef](#)]
40. Silva, L.G.; Weber, G. Mesoscopic model confirms strong base pair metal mediated bonding for T–Hg²⁺–T and weaker for C–Ag⁺–C. *Chem. Phys. Lett.* **2022**, *803*, 139847. [[CrossRef](#)]
41. Freeman, G.S.; Hinckley, D.M.; de Pablo, J.J. A coarse-grain three-site-per-nucleotide model for DNA with explicit ions. *J. Chem. Phys.* **2011**, *135*, 165104. [[CrossRef](#)]
42. Florescu, A.; Joyeux, M. Thermal and mechanical denaturation properties of a DNA model with three sites per nucleotide. *J. Chem. Phys.* **2011**, *135*, 085105. [[CrossRef](#)] [[PubMed](#)]
43. Sayar, M.; Avşaroğlu, B.; Kabakçoğlu, A. Twist-writhe partitioning in a coarse-grained DNA minicircle model. *Phys. Rev. E* **2010**, *81*, 041916. [[CrossRef](#)] [[PubMed](#)]
44. Sambriski, E.J.; Ortiz, V.; de Pablo, J.J. Sequence effects in the melting and renaturation of short DNA oligonucleotides: Structure and mechanistic pathways. *J. Phys. Condens. Matter* **2009**, *21*, 034105. [[CrossRef](#)]
45. Zhang, F.; Collins, M.A. Model simulations of DNA dynamics. *Phys. Rev. E* **1995**, *52*, 4217–4224. [[CrossRef](#)]
46. Drukker, K.; Wu, G.; Schatz, G.C. Model simulations of DNA denaturation dynamics. *J. Chem. Phys.* **2001**, *114*, 579–590. [[CrossRef](#)]
47. Ouldridge, T.E.; Louis, A.A.; Doye, J.P.K. Structural, mechanical, and thermodynamic properties of a coarse-grained DNA model. *J. Chem. Phys.* **2011**, *134*, 085101. [[CrossRef](#)]

48. Wong, K.Y.; Pettitt, B.M. The pathway of oligomeric DNA melting investigated by molecular dynamics simulations. *Biophys. J.* **2008**, *95*, 5618–5626. [[CrossRef](#)] [[PubMed](#)]
49. Lomzov, A.A.; Vorobjev, Y.N.; Pyshnyi, D.V. Evaluation of the Gibbs free energy changes and melting temperatures of DNA/DNA duplexes using hybridization enthalpy calculated by molecular dynamics simulation. *J. Phys. Chem. B* **2015**, *119*, 15221–15234. [[CrossRef](#)]
50. Kundu, S.; Mukherjee, S.; Bhattacharyya, D. Melting of polymeric DNA double helix at elevated temperature: A molecular dynamics approach. *J. Mol. Model.* **2017**, *23*, 1–10. [[CrossRef](#)]
51. Chen, X.; Karpenko, A.; Lopez-Acevedo, O. Silver-mediated double helix: Structural parameters for a robust DNA building block. *ACS Omega* **2017**, *2*, 7343–7348. [[CrossRef](#)] [[PubMed](#)]
52. Mistry, L.; Waddell, P.G.; Wright, N.G.; Horrocks, B.R.; Houlton, A. Transoid and cisoid conformations in silver-mediated cytosine base pairs: Hydrogen bonding dictates argentophilic interactions in the solid state. *Inorg. Chem.* **2019**, *58*, 13346–13352. [[CrossRef](#)] [[PubMed](#)]
53. Espinosa Leal, L.A.; Karpenko, A.; Swasey, S.; Gwinn, E.G.; Rojas-Cervellera, V.; Rovira, C.; Lopez-Acevedo, O. The role of hydrogen bonds in the stabilization of silver-mediated cytosine tetramers. *J. Phys. Chem. Lett.* **2015**, *6*, 4061–4066. [[CrossRef](#)] [[PubMed](#)]
54. Hanwell, M.D.; Curtis, D.E.; Lonie, D.C.; Vandermeersch, T.; Zurek, E.; Hutchison, G.R. Avogadro: An advanced semantic chemical editor, visualization, and analysis platform. *J. Cheminform.* **2012**, *4*, 4–17. [[CrossRef](#)] [[PubMed](#)]
55. Van Der Spoel, D.; Lindahl, E.; Hess, B.; Groenhof, G.; Mark, A.E.; Berendsen, H.J. GROMACS: Fast, flexible, and free. *J. Comput. Chem.* **2005**, *26*, 1701–1718. [[CrossRef](#)] [[PubMed](#)]
56. Ivani, I.; Dans, P.D.; Noy, A.; Pérez, A.; Faustino, I.; Hospital, A.; Walther, J.; Andrio, P.; Goñi, R.; Balaceanu, A.; et al. Parmbsc1: A refined force field for DNA simulations. *Nat. Methods* **2015**, *13*, 55. [[CrossRef](#)]
57. Li, P.; Song, L.F.; Merz, K.M. Systematic Parameterization of Monovalent Ions Employing the Nonbonded Model. *J. Chem. Theory Comput.* **2015**, *11*, 1645–1657. [[CrossRef](#)]
58. Filho, E.D.; Ruggiero, J.R. H-bond simulation in DNA using a Harmonic Oscillator Isospectral Potential. *Phys. Rev. E Stat. Phys. Plasmas Fluids Relat. Interdiscip. Top.* **1997**, *56*, 4486–4488. [[CrossRef](#)]
59. Zou, Y.; Xiang, S.; Dai, C. Investigation on the efficiency and accuracy of methods for calculating melting temperature by molecular dynamics simulation. *Comput. Mater. Sci.* **2020**, *171*, 109156. [[CrossRef](#)]

Disclaimer/Publisher's Note: The statements, opinions and data contained in all publications are solely those of the individual author(s) and contributor(s) and not of MDPI and/or the editor(s). MDPI and/or the editor(s) disclaim responsibility for any injury to people or property resulting from any ideas, methods, instructions or products referred to in the content.